BBA - Biomembranes 1860 (2018) 1216–1230

Contents lists available at ScienceDirect

BBA - Biomembranes

journal homepage: www.elsevier.com/locate/bbamem

Insertion of Dengue E into lipid bilayers studied by neutron reflectivity a molecular dynamics simulations

Juan M. Vanegas[a,1,2], Frank Heinrich[b,c,2], David M. Rogers[a,3], Bryan D. Carson[a], Sadie La Bau Briana C. Vernon[a], Bulent Akgun[b,4], Sushil Satija[b], Aihua Zheng[d,5], Margaret Kielian[d], Susan B. Rempe[a], Michael S. Kent[a,*]

[a] Sandia National Laboratories, Albuquerque, NM, United States
[b] National Institute of Standards and Technology Center for Neutron Research, Gaithersburg, MD, United States
[c] Department of Physics, Carnegie Mellon University, Pittsburgh, PA, United States
[d] Department of Cell Biology, Albert Einstein College of Medicine, Bronx, NY, United States

ARTICLE INFO

Keywords:
Dengue virus
Membrane fusion
Envelope protein
Fundamental interactions
Neutron reflectivity
Molecular dynamics simulations

ABSTRACT

The envelope (E) protein of Dengue virus rearranges to a trimeric hairpin to med target membranes, which is essential for infectivity. Insertion of E into the target m and possibly also to disrupt local order within the membrane. Both aspects are likely of insertion, orientation of the trimer with respect to the membrane normal, and between trimer and membrane. In the present work, we resolved the depth of inse fundamental interactions for the soluble portion of Dengue E trimers (sE) associat membranes of various combinations of 1-palmitoyl-2-oleoyl-*sn*-glycero-3-phosphoc 2-oleoyl-*sn*-glycero-3-phospho-rac-glycerol (POPG), 1-palmitoyl-2-oleoyl-*sn*-glyc (POPE), and cholesterol (CHOL) by neutron reflectivity (NR) and by molecular dyna results show that the tip of E containing the fusion loop (FL) is located at the interfac chains of the outer leaflet of the lipid bilayers, in good agreement with prior predicti that E tilts with respect to the membrane normal upon insertion, promoted by eith CHOL. The simulations show that tilting of the protein correlates with hydrogen bon and arginines located on the sides of the trimer close to the tip (K246, K247, headgroups. These hydrogen bonds provide a major contribution to the membrane destabilize the target membrane.

1. Introduction

All enveloped viruses have a dedicated protein that promotes fusion between viral and host membranes [1–3]. Fusion proteins are critical for infectivity and are targets of therapeutic intervention. All fusion functions include anchoring into the host meml support the high-energy membrane bending th fusion stalk; [4,6–8] promoting positive curva brane and dimple formation, or promoting n quired to form a fusion stalk; [1,4,9,10] or disr

proteins have a hydrophobic peptide sequence that inserts into the host membrane although the sequences and structures vary considerably among the different enveloped viruses. Although many structures have been solved, the functional mechanisms of fusion proteins and their hydrophobic peptides are still under considerable debate [4,5]. Possible

* Corresponding author.
E-mail address: mskent@sandia.gov (M.S. Kent).
[1] Current address: Department of Physics, University of Vermont, United States.
[2] JMV and FH contributed equally to this work.
[3] Current address: Department of Chemistry, University of South Florida, United States.
[4] Current address: Bogazici University, Istanbul, Turkey.
[5] Current address: Institute of Zoology, Chinese Academy of Sciences, Beijing, China.

membrane, thereby promoting fusion [16,17]. More work is needed to understand fully the detailed mechanisms by which such proteins promote fusion and the roles of their fusion peptides.

In the present work, we studied the fundamental interactions of the soluble portion of the envelope protein of Dengue virus serotype 2 with lipid membranes. Dengue virus (DV) is a flavivirus that is endemic to tropical and subtropical regions of the world [18,19]. The envelope protein (E) is comprised of three domains and is arranged as a head-to-tail dimer in the mature virus, but reorganizes into head-to-head trimers upon exposure to low pH within endosomes [20]. Residues 98-111 comprise the fusion loop (FL) at the tip of the trimer that inserts into the target membrane. While much prior work has focused on the importance of the FL, we show below that positively-charged arginine and lysine residues (R73, K246 and K247) located on the sides of the trimer (within 10 Å from the FL) are also important in the interaction of Dengue E with the target membrane, as suggested recently for the flavivirus St. Louis encephalitis virus [21]. Our simulations indicate that hydrogen bonds formed between these residues and phosphates in the lipid headgroups provide substantially more enthalpic interaction energy than the interaction of the fusion loop with the membrane.

A great deal of evidence indicates that the sequence of the FL of DV is important for fusion, strongly suggesting that the structure, positioning, and specific interactions of the fusion loop within the bilayer are crucial. The amino acid (AA) sequence of the FL is highly conserved among flaviviruses (Fig. S1) [8,14,15,22]. Mutational studies have shown that fusion efficiency is extremely sensitive to various residues in the FL, especially W101, L107, and F108 [7,8,23]. However, the basis for the extreme sensitivity to these aspects is not yet clear. Residues W101, L107, and F108 have been collectively referred to as a hydrophobic anchor [6–8]. But considering membrane binding energies of a large number of peripheral membrane-associated proteins [24] it is surprising that a protein that associates only with the headgroup region of the outer leaflet and inserts only a few hydrophobic residues into the lipid tails will bind irreversibly and remain anchored in the membrane in the presence of large membrane bending stresses that must occur during formation of the fusion stalk. For comparison, a single myristate group (14 carbons) is known to be insufficient to provide stable anchoring to lipid membranes [25–27]. While hydrophobic interactions between the FL and the lipid membrane may contribute to anchoring, the modest interaction energy afforded by three strongly hydrophobic residues (nine in the trimer) and conservation of the structure and sequence of the FL suggests a critical role beyond this.

of the host membrane to facilitate mixing w
[1,4,11]. With regard to the latter, prior studie
peptides lower the rupture tension of membr

simulations have suggested that the fusion p
motes splaying of lipid tails, such that one tail

insertion, the orientation of sE with respect to
and the fundamental interactions that occur be
The results show that positively-charged lysir
arginine R73 in the vicinity of the FL contril
interaction. In particular, K246 and K247 each
bonds with phosphates of lipid headgroups tha
upon insertion. These hydrogen bonds are pr
CHOL, but the effect is much stronger for AL.
these hydrogen bonds play an important role i
along with the FL.

2. Materials and methods

2.1. Materials

POPC, POPG sodium salt, POPE, and CHC
Avanti Polar Lipids. The HC18 (*Z*-2
3,6,9,12,15,18,22-heptaoxatetra-cont-31-ene-1
pound was synthesized at NIST as previously r

2.2. Expression and purification of DV2 sE

The DV2 construct (strain NGC) used in th
and E ectodomain residues 1-395 with single
has been described in detail elsewhere [35].
pressed in S2 cells as follows. S2 cells were grov
(Thermo Hyclone). Initially, we used altern
(Insectagro-DS2, Life Technologies) but obtaine
relative to other media and poor protein yield
baffled flasks containing 600 mL of mediu
3–6 × 10^6 cells per mL and copper sulfate w
centration of 1 mM on culture day 0. On days
was harvested by centrifugation at 13,000 × g
batch, a total of 8 L of clarified and 0.2 µm-f
then concentrated to 1 L using Vivaflow 200 c
10,000 Da cutoff). Egg white avidin (Life Techr
to the supernatant at a final concentration o
biotin that would interfere with purification,
adjusted to 8.0 using 0.5 M NaOH with rapi
During our efforts, we determined that bu
necessary for binding to streptactin and genera
crystalline precipitate that clogged the affinit

As is common for enveloped viruses, fusion of flaviviruses has been shown to depend upon the lipid composition of the target membrane. In particular, fusion depends strongly on anionic lipids (AL) and, in the absence of AL, on CHOL [28–31]. Interestingly, the dependence of fusion on CHOL occurs despite lack of a strong association between CHOL and sE [32]. While the viral membrane composition can also impact fusion and will differ for virus produced in different types of cells such as vertebrate and insect cells, we focus here on the composition of the endosomal membrane and its impact on fusion.

In this work, we studied the structure and fundamental interactions of Dengue sE inserted into membranes of 70:30 1-palmitoyl-2-oleoyl-*sn*-glycero-3-phosphocholine (POPC): 1-palmitoyl-2-oleoyl-*sn*-glycero-3-phospho-rac-glycerol (POPG), 49:21:30 POPC:POPG:CHOL, and 49:21:30 POPC:1-palmitoyl-2-oleoyl-*sn*-glycero-3-phosphoethanolamine (POPE):CHOL by neutron reflectivity (NR). We also studied 70:30

was then passed over two 1 mL streptactin colu
a flow rate of 1 mL/min. Columns were washe
then eluted using 5 mM desthiobiotin (Sigma

exchange (1:100–1:500) and concentration we
ultrafiltration and TAN buffer (20 mM t
130 mM NaCl). Purified protein in TAN buffe
spectrophotometer (NanoDrop2000) using
weight of 46,906 Da and molar absorption
Aliquots were stored at −80 °C.

2.3. Preparation of tethered lipid bilayer membra

Adsorption of sE to tethered bilayer lipid
studied by NR. tBLMs were prepared on HC
layer (SAM) coated 2(diameter Silicon wafer

NaCl, pH 8.0) and vortexed for 1 min. Two cycles of hydration and vortex agitation were performed to release all lipids from the vial wall. The liposomes thus formed (2.5 mg/mL) were injected into the measurement cell containing a gold-coated wafer with tethering HC18-SAM, incubated for a minimum of 1 h, and then exchanged with a low salt TAN buffer (20 mM triethanolamine, 50 mM NaCl, pH 8.0).

2.4. Preparation of lipid monolayers at the air-water interface

Adsorption of sE to Langmuir monolayers of either 100% DPPG or a 70:30 mol% mixture of DPPC and DPPG was studied by NR and X-ray reflectivity (XR). The lipids were spread from a mixture of chloroform and methanol on the surface of 20 mM MES buffered H_2O subphase (pH 5.5, 130 mM NaCl) held within a Teflon trough (70 mm × 70 mm × 2 mm). After allowing the chloroform and methanol to evaporate, the surface layer was compressed to the target pressure by a movable barrier. Sufficient lipid was deposited such that after reaching the target pressure the barrier remained outside of the footprint of the X-ray or neutron beam. After collecting XR or NR data for the lipid monolayer alone, sE was then injected into the subphase underneath the lipid monolayer. For the case of a 70:30 mol% mixture of DPPC and DPPG, a stable surface layer of sE bound to the lipid monolayer could not be attained, despite exploring various combinations of surface pressure and sE concentration. However, a stable surface layer of membrane-bound sE resulted for the case of 100% DPPG at a surface pressure 30 mN/m. In that case sE was injected at a concentration of 1.2 μM. After waiting several hours for adsorption to be completed, X-ray reflectivity scans were collected. The trough was maintained at 20 ± 2 °C.

2.5. Background on neutron and X-ray reflectivity

NR and XR are analogous to the more familiar small angle scattering (SAS) methods used to study the structure of proteins and protein complexes in solution [37]. However, in contrast to SAS, NR and XR can be used to study membrane-bound proteins [38]. NR and XR involve measuring the ratio of reflected intensity to incident intensity as a function of momentum transfer $q_z = 4\pi\sin\theta/\lambda$, where θ is the angle of incidence and λ is the wavelength. The form of this curve is determined by the profile of the in-plane averaged neutron or X-ray scattering length per volume, or scattering length density (SLD), normal to the surface [39]. The neutron or x-ray SLD is directly related to the atomic

the known chemical components, called comp
[42]. This method constrains the fits to plaus
and increases the precision with which molec
localized within the interfacial structure. Mol
tein structure, derived from a crystal structure
ories, can be incorporated into the fitting a
molecular structure into a stack of slabs no
calculating the SLD for each slab from the
density. The volume fraction, vertical positio
structure, and tilt angle of the protein can th
with the distributions of the lipid componen
multiple contrast conditions can be fit simult
improves the ability to resolve the distributi
nents.

2.6. NR measurements

NR measurements of sE adsorption to tLBM
NG7 reflectometer at the NIST Center for Ne
Reflectivity curves were recorded for mon
$0 \le q_z \le 0.25$ Å^{-1}. For each measurement, ad
were obtained after 5–7 h. The flow cell allo
change; therefore, subsequent measurements
same sample area. The entire flow cell was m
perature (RT). After in situ completion of t
collected with H_2O buffer (20 mM TAN, 130 m
in the measurement cell. Buffer exchange was a
10 mL of buffer through the cell (volume ~1.3
experiments involving Dengue sE were perfor
In the first, a 2 mL solution of 1 μM sE in buffe
into the measurement cell using a syringe a
several hours during which short NR scans w
the level of adsorption. This was repeated thr
adsorption occurring in each case. Following
1 μM sE, final scans were collected. This pro
PC:PG membrane. In the second protocol, fol
data for the tBLM in H_2O and D_2O buffer, a 2
concentration of sE (3.4 μM for PC:PG:CHOL an
in pH 5.5 buffer was injected into the measurer
For each of these cases, 5% PEG 400 was incl
tion of protein and non-specific adsorption of p
Short NR scans were collected until adsorption

surface [39]. The neutron or x-ray SLD is directly related to the atomic composition and the density of the reflecting body. (Since X-ray SLD is proportional to the electron density, the latter is typically reported rather than the SLD). Therefore, for a protein bound to a planar lipid membrane, NR and XR determines the distribution of amino acid residues normal to the membrane (averaged in-plane) with resolution comparable to that of the corresponding SAS methods (typically 10–20 Å). While the amino acid distribution within a protein is determined to only low resolution, the vertical position of a protein relative to the membrane is determined to a much higher precision [40]. Manipulating the contrast between components within a structure is integral to neutron scattering methods. For organic materials this is readily accomplished using the very different neutron SLD of hydrogen and deuterium.

While some information can be obtained from reflectivity data by inspection, such as determining thicknesses from fringe spacings, a

Short NR scans were collected until adsorption was then exchanged with D_2O buffer, and a Then the cell was exchanged with H_2O buffe collected.

The 1D-structural profile along the lipid b NR scans consisted of a stratified slab model fo a continuous distribution model for the tBLM Hermite spline for the model-free envelope dividual slabs were implemented for the bulk the chromium, and the gold layer. Fit param neutron scattering length density for each la silicon. One global roughness fit parameter ap terfaces. Individual sub-molecular groups in tinuous distribution model are: β-mercapt polyethylene glycol (PEG) chains, tether gly proximal and substrate distal PG and PE hea

optimization. Fit parameters for each control point are the volume occupancy of the envelope and the deviation from a position defined by equidistant control points throughout the spline. Over the extension of the spline, a constant neutron SLD is applied, which is a function of the bulk solvent SLD taking into account proton exchange of the protein with the bulk solvent. Since reflectivity measures the profile normal to the interface (averaged in-plane), the volume distributions of the various components at each depth through the interface are expressed as cross-sectional areas. The maximum value of the cross-sectional area equals the global area per molecule of that component.

To determine the orientation of the protein at the lipid bilayer, we performed additional fits using rigid structural models for the protein [44]. The structure 1OK8.pdb was used along with a modified structure in which the monomers are splayed to an angle of roughly 52°, as suggested by Klein et al. in the absence of a zipped-up stem region [45]. We refer to the latter structure as “open form.” An animation showing the two structures is provided in the Supporting information (Fig. S2). Both structures were aligned with their largest principal axis along the bilayer normal, and with the membrane-binding interface toward the bilayer. The resulting structures define the respective (0°, 0°) orientation. For modeling the NR data, two continuous fit parameters, equivalent to the two Euler angles (β, γ), describe the final orientation of the protein at the interface. Every orientation (β, γ) can be obtained by extrinsic rotations of the protein around the axes of the bilayer coordinate system. First, the protein is rotated by γ about the membrane normal, or the *z*-axis. Second, the protein is rotated by β about the *x*-axis, which is in plane with the membrane. The third Euler angle would correspond to a third extrinsic rotation around the *z*-axis, but NR is invariant to this orientation. The fit allows for orientations within $0° \leq \beta \leq 90°$ and $0° \leq \gamma < 360°$. Data modeling and optimization of model parameters were performed using the ga_refl and Refl1D software packages developed at the NCNR [36]. Optimization of model parameters was achieved by using a differential evolution Markov chain. All reflectivity curves of one data set were fit simultaneously to the same model, sharing fit parameters, for example, for the solid substrate. A Monte Carlo simulation or analysis of the Monte Carlo Markov chain was used to determine the fit parameter confidence limits, avoiding over-parameterization.

NR measurements of sE adsorption to Langmuir monolayers were performed at the NG7 reflectometer at the NIST Center for Neutron Research (NCNR). Reflectivity curves were recorded for momentum

2.8. MD simulations

The DV soluble E trimer was simulated ba the crystal structure (PDBID: 1OK8 [6], residue truncated model of the sE trimer (residues 5 used to study interactions of the tip and fusion lipid membranes. The truncated sE model is le the full sE trimer and significantly lowers the c costs. The truncation point was chosen to ke (C60-C121, C92-C116, and C74-C105) that hel of the reduced model. The full-length and tr each simulated in solution (including 130 m compare the structural validity of the trunc states for amino acids in both sE models we results from PROPKA [46] analysis of the crys

The truncated sE trimer was simulated systems with varying ratios of POPC, POPE, PC:PG bilayer was composed of 358 PC an PC:PG). The PC:PE:CHOL bilayer was compose 216 CHOL lipids (1:1:1 PC:PE:CHOL). The PC:P of 256 PC and 256 PE lipids (1:1 PC:PE). Each by random lateral (in the membrane plane) d ponents in each leaflet, followed by water sc and equilibrated for 400 ns. Two truncated sE one side of each lipid membrane, with the fus protein tip within contact distance of the lipi cipal axis of each truncated sE trimer was in membrane normal so that the protein was “up to the membrane plane. The two proteins wer that the distance between closest atoms was > the water layer was adjusted in each case to truncated sE trimer was ~2.0 nm from the othe across the periodic boundary. Ion concentratio system to have a 130 mM NaCl concentratio systems were simulated for 600–700 ns, as ne

For the PC:PG and PC:PE:CHOL membran tilt” simulation was run in which the truncated to a perpendicular orientation with respect to t This condition was achieved by applying a h constant of 1000 kJ × mol $^{-1}$ × nm^2) to the a V97, D98, I232 and Q233 of each monomer i

transfer values $0 \leq q_z \leq 0.25\ \text{Å}^{-1}$.

2.7. XR measurements

XR measurement of sE bound to a Langmuir monolayer of 100% DPPG was performed using an X-ray reflectometer (Bruker, D8 Advance) employing Cu K_α radiation at NCNR/NIST (Gaithersburg, MD). The copper source was operated at 40 kV and 40 mA, and the wavelength was 0.154 nm. The beam width was 10 mm and the beam height was 0.1 mm.

For the case of a monolayer of 100% DPPG, the XR data were analyzed using the Ga_refl program based on the optical matrix method. Analyses were performed with free form models involving a small number of slabs. The free form models consisted of one layer each for the lipid tails and the lipid headgroups, and one layer for the protein. This was sufficient to achieve a good fit to the data. Since no insertion

while allowing free motion in z.

Protein atoms were modeled with the GR

[47] while the lipid atoms where modele
GROMOS 43A1-S3 parameter set of Chiu et a
eled with the SPC/E 3-point parameter set [49
conducted with the GROMACS 4.5.7 software
was held constant at 1 atm for all systems w
barostat (isotropically for protein in solution a
membrane systems). Temperature was held at
over thermostat for all simulations to match th
for the fixed-tilt systems. In those systems the
310 K to match physiological conditions. Hy
termined based on a distance criteria of 3.5 Å b
and acceptor atoms only, and no angle criter
splay angle with respect to the membrane no
measuring the angle of the vector starting at t

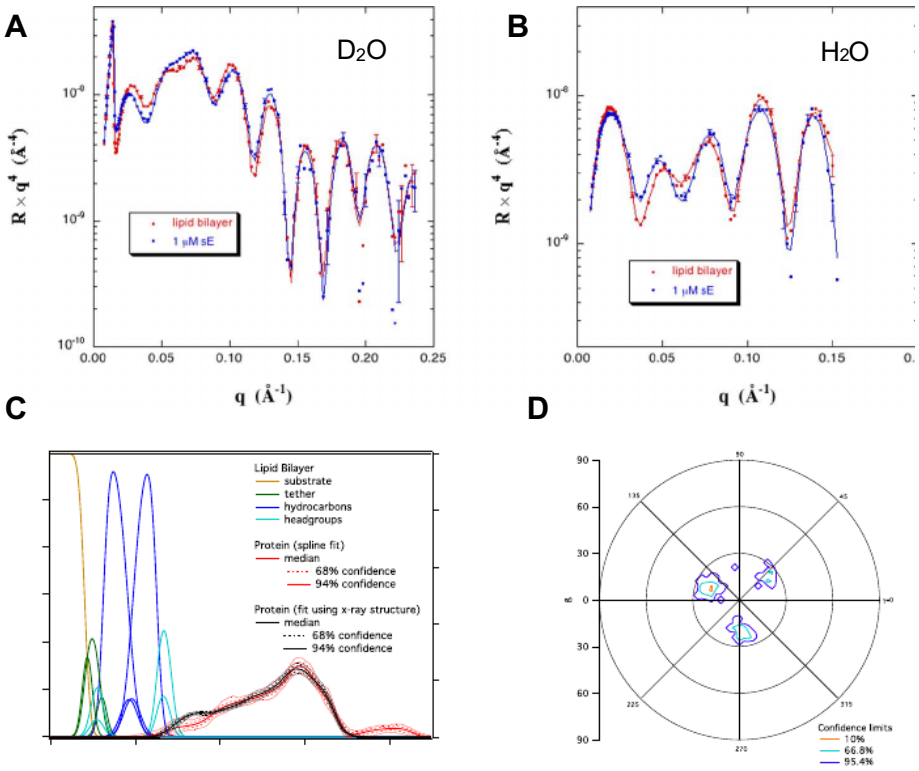

Fig. 1. NR data for E bound to 70:30 PC:PG tethered lipid bilayer in A) D $_2$O and B) H_2O. Also shown are C) volume occupancy profiles for the differen distributions of sE for the best fits.

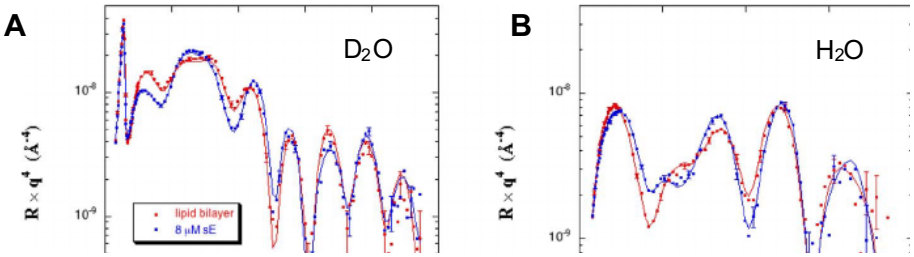

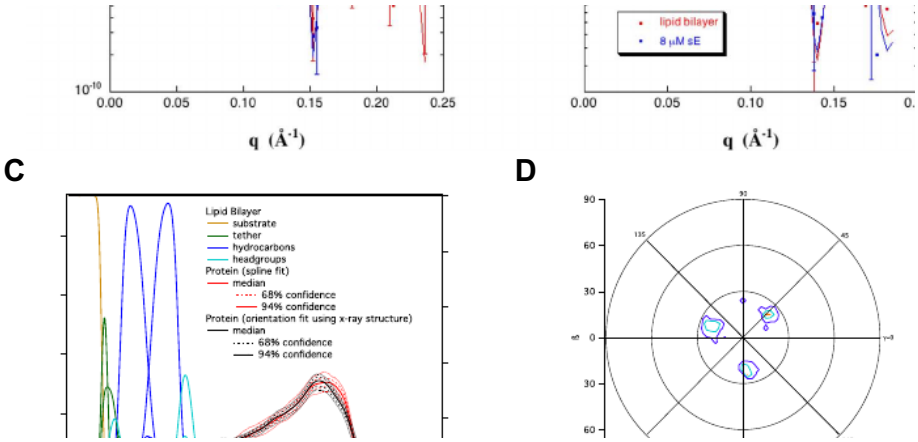

Table 1
Summary of results from fitting the NR data.
Median fit parameters and 68% confidence limits.

Parameter	Spline fit	Fixed orientation x-ray structure fit with closed-form	Orientation fit with the closed-form x-ray structure	Orientatio ray struct
70:30 PC:PG				
Bilayer roughness, σ/Å	2.4 ± 0.3	2.9 ± 0.3	2.7 ± 0.3	2.7 ± 0.2
Area per lipid with protein at the interface/Å^2	62.4 ± 1.6	67.1 ± 1.4	63.3 ± 1.9	63.0 ± 1.
Penetration into lipid bilayer	n/a	16.5 ± 0.6	11.0 ± 1.9	16.6 ± 3.
Amount of surface-associated protein/ (Å^3/Å^2)	13.5 ± 0.7	11.6 ± 0.4	14.1 ± 0.6	13.6 ± 1.
χ^2	1.15	1.20	1.12	1.22
49:21:30 PC:PE:CHOL				
Bilayer roughness, σ/Å	3.0 ± 0.3	2.7 ± 0.2	2.5 ± 0.2	2.6 ± 0.2
Area per lipid with protein at the interface/Å^2	55.7 ± 1.5	48.8 ± 0.8	46.9 ± 1.0	48.2 ± 0.
Penetration into lipid bilayer	n/a	14.3 ± 0.5	8.9 ± 1.4	15.4 ± 2.
Amount of surface-associated protein/ (Å^3/Å^2)	20.7 ± 1.2	19.0 ± 0.6	17.4 ± 0.9	19.4 ± 0.
χ^2	1.18	1.27	1.06	1.37
49:21:30 PC:PG:CHOL				
Bilayer roughness, σ/Å	2.5 ± 0.3	2.7 ± 0.2	2.3 ± 0.2	2.4 ± 0.2
Area per lipid with protein at the interface/Å^2	58.3 ± 1.5	52.2 ± 1.2	49.0 ± 1.0	51.7 ± 1.
Penetration into lipid bilayer	n/a	17.4 ± 0.5	9.6 ± 1.5	21.8 ± 1.
Amount of surface-associated protein/ (Å^3/Å^2)	26.4 ± 0.9	23.3 ± 0.6	23.5 ± 0.7	24.8 ± 0.
χ^2	1.07	1.74	1.27	1.26

best-fit model in terms of the volume occupancy profiles of the various components and the angular distribution of sE, where the closed form crystal structure of the sE trimer was used in the fits. Corresponding data for sE inserted into a 49:21:30 PC:PE:CHOL tBLM are shown in Fig. 2. Data for a 49:21:30 PC:PG:CHOL tBLM are provided in Fig. S3. Best fits were independently determined using a free-form Hermite spline that makes no assumptions about the shape of the volume occupancy profile, and also using the X-ray crystal structures of the sE trimer within a rigid body modeling approach. Two crystal structures for the sE trimer have been published, which we refer to as the closed and open forms [6,45]. Both forms were used in the fitting. The fitting results are summarized in Table 1. A complete listing of fit parameters

binding of sE.

3.2. NR and XR studies of sE adsorption to lipid m interface

Adsorption of sE to Langmuir monolayers o 70:30 mol% mixture of DPPC and DPPG was a XR. For the case of a 70:30 mol% mixture of D surface layer of sE bound to the lipid monolay despite exploring various combinations of s concentration. Rather, under conditions for w

is given in the Supporting information (Table S1).

sE trimer structures were used in the fitting because prior work has shown that sE forms trimers upon insertion into lipid membranes and that nearly all of the inserted protein is in the trimer form [51]. The measurements were performed after incubation at pH 5.5 for > 2 h. This is more than enough time for trimerization of membrane-bound sE [31,32] and for the final form with domain III folded back against domain II to be reached [28,33].

For 70:30 PC:PG and 49:21:30 PC:PE:CHOL, better fits (as measured by the χ^2 values) resulted from using the closed form structure, whereas comparable quality fits were obtained for the open and closed trimer structures in the case of 49:21:30 PC:PG:CHOL. The fitting results show that the final state of the inserted protein is similar for the three membrane compositions. E inserts such that the FL at the tip of the protein coincides with the interface between the lipid headgroups and the hydrophobic tails. The depth of insertion of sE for the different

curred as detected by backward movement
continued until the barrier reached the back o

the NR or XR data indicated that sE had inse
layer and was exposed to the air interface, rat
the lipid layer into the subphase as observe
Figs. 1 and 2. Since the presence of the air inte
adsorption and insertion process, we conclude
layers are not an adequate mimic of the outer
with respect to studying the membrane-insert
ever, for the case of 100% DPPG, a stable surf
was obtained. In that case, virtually no mov
sulted, indicating little or no insertion of sE. X
case are shown in Fig. 3 along with the fitti
density profile is qualitatively different from tl
into bilayers shown in Figs. 1 and 2. The res
single layer for the protein below the lipid head
layer) with an average thickness of 38 Å follo

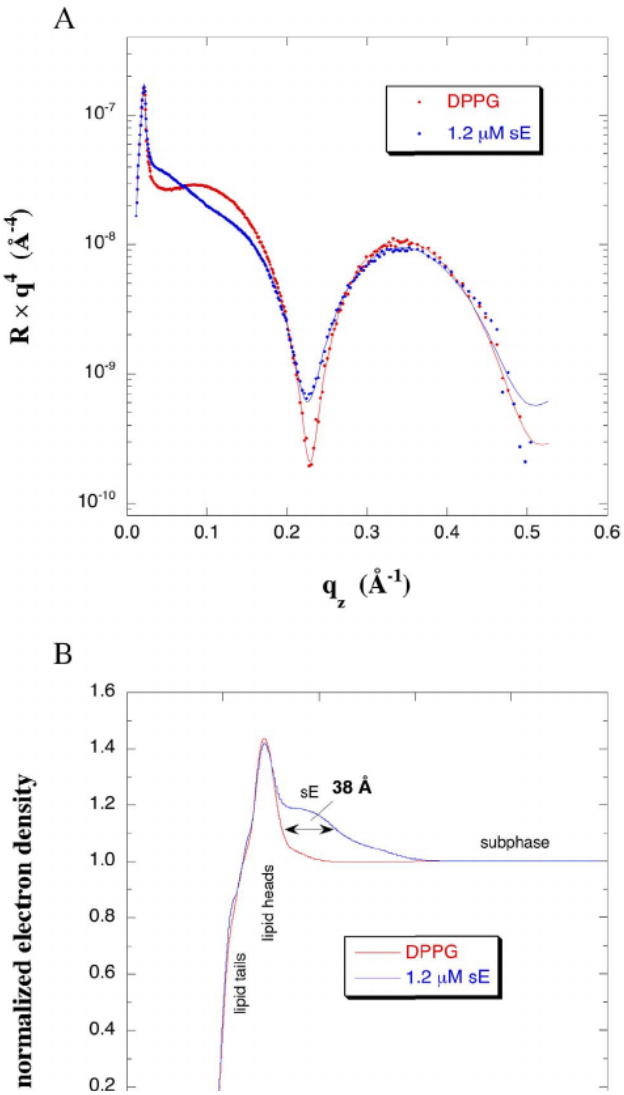

the full sE trimer (Fig. 4). While the TT is slig
the truncation regions, the structure of ea
(Fig. 4C) as well as the FL region for the TT re
structure, as shown in the root-mean-squared

Two distinct TT structures, each taken f
brated simulations, were brought into conta
lipid membranes (512-648 lipids, see Meth
compositions (1:1 PC:PE, 1:1:1 PC:PE:CHOL,
TT was placed in a vertical orientation (long a
membrane plane and FL in contact with lipid
simulated for 600–700 ns. During each simu
cases adopted a tilted orientation with respect
dependent changes in the tilt angle, hydrogen
sertion are shown in Fig. 5 for the two trim
membrane compositions. The depth of inserti
tance from the center of mass of residue W
center of mass of the phosphate groups of nei
contact with the protein). The magnitude of t
PC:PE:CHOL and PC:PG, but considerably wea
is strongly correlated with the number of hydr
establishes with the neighboring lipids. For e
tion, the largest number of hydrogen bonds oc
oxygens of the lipid headgroups (Fig. 6). The P
a lesser extent the PE NH_3, also provide a signi
overall protein-lipid hydrogen bonding (Fig. 6
the TTs increases beyond 20–30°, the Lys and
iphery of the protein (especially K246, K247
establish a significant number of hydrogen b
drogen bonds, Fig. 7). Most of the lysines tha
groups form 2-3 hydrogen bonds with the ph
picted in Fig. 7E. Interestingly, K110 in the
forms hydrogen bonds with the lipids due to th
the interface of the three monomers and form
nearby protein residues instead.

While there is a preference for TT to hyc
lipids over PC (Fig. S3), the ratios of protein-li
not show any clear pattern of clustering or lipi
proteins. The TTs have few interactions with c
to the fact that cholesterol is located in the lipi
extend into the lipid headgroups (Figs. S4 and

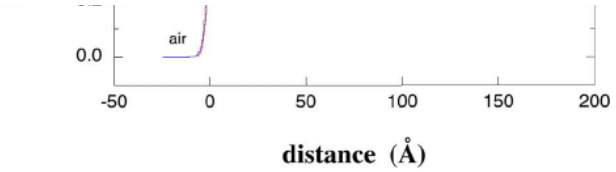

Fig. 3. A) X-ray reflectivity data and B) fitted electron density profiles for sE binding to a monolayer of 100% DPPG in a Langmuir trough. The profile is entirely different from that in Figs. 1-2, and shows that in the unrealistic case of a membrane of 100% AL the electrostatic interactions with positively-charged residues exposed on the surface of sE are sufficiently strong to cause the protein to adsorb in a side-on orientation.

3.3. Simulations of sE trimer with lipid membranes

We characterized the molecular level interactions between Dengue sE trimer and lipid membranes with atomistic MD simulations. The large size of the trimeric protein (> 1000 AAs with a length > 100 Å,

extend into the lipid headgroups (Figs. 3 and

conserved (Fig.S1) W101 is located in the fusio
bottom left panel) and penetrates significantl

PC:PE:CH membrane compared to the othe
bottom panels). This deeper insertion is facilita
cholesterol molecules (Fig. S5). Increased tilt a
the PC:PG and PC:PE:CHOL membranes may
deeper insertion of W101 compared to PC:PE

Since the protein-membrane interactions
trimers, we wondered if the membrane would
not free to tilt. To answer this question, we sir
PC:PG and PC:PE:CHOL membranes while fix
Section 2.8 for details) of each TT to rema
membrane plane (tilt angle < 10°, Fig. 8). Th
hydrogen bonding for the PC:PG fixed-orientati
large deformation of the membrane as the lipic
the TT (Fig. 8B). The highest total numb
(127 ± 7) between the vertically fixed TT a

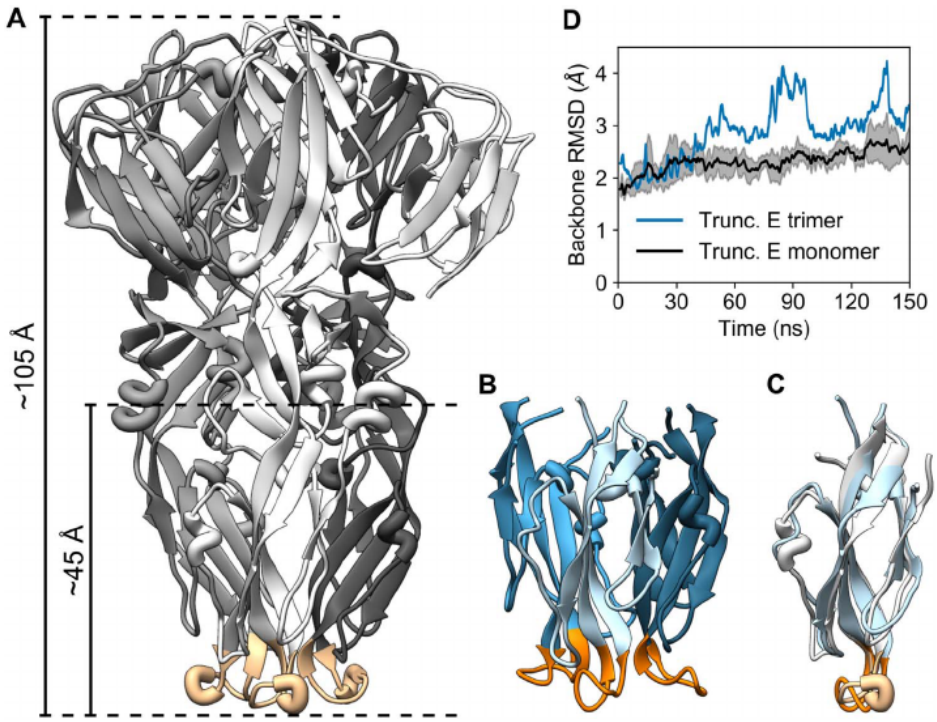

Fig. 4. Truncated E trim
solution. A) Crystal str
truncated model (bott
sion loop (tan region).
after 150 ns simulation
cated monomer (simu
crystal structure of com
squared deviation of tr
relative to the crystal st
and average of the t
compared to the crysta

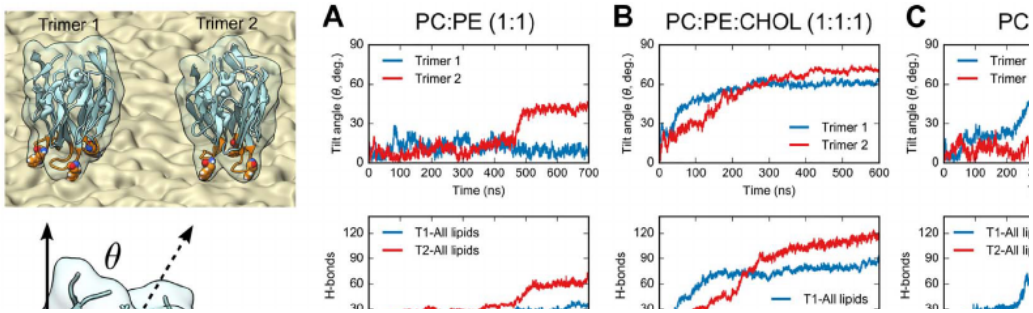

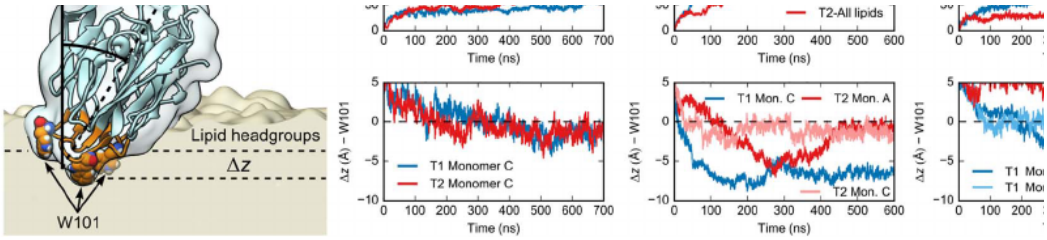

Fig. 5. Tilt angle, number of hydrogen bonds, and W101 depth of insertion (Δz, with respect to surrounding lipid headgroups) of simulated truncated PC:PE:CHOL, and (C) PC:PG lipid membranes as a function of time. Truncated E trimers positioned in contact with PC:PE:CHOL and PC:PG lipid bilayers t = 0) over time. The bottom panels only show data for W101 residues that penetrate below the headgroup region for clarity. Number of hydrogen bon correlated with tilt angle and membrane composition.

with neighboring lipids (Fig. 8F).

To further characterize the protein-membrane interactions, we computed the approximate interaction energies due to van de Waals and short range Coulomb (up to 1 nm away) forces between each TT

a larger number of FL residues in contact wi lower tilt. When the protein is fixed in a ver teraction energy for the PC:PG case (−1707 k to that of the free tilt case, as expected giv

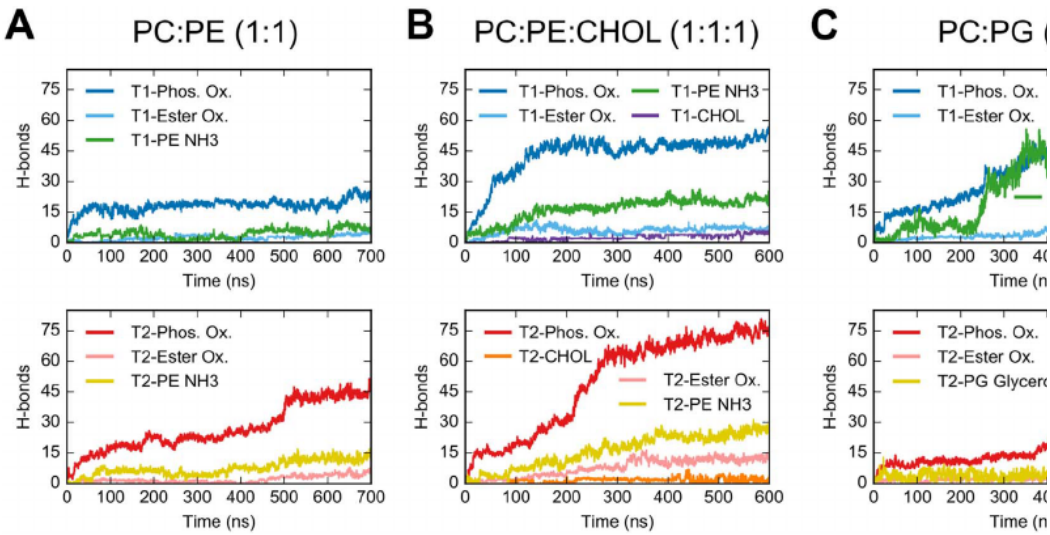

Fig. 6. Number of hydrogen bonds between the truncated E trimers and the various chemical moieties in the lipid headgroups (phosphate oxygens, este ethanolamine NH_3, cholesterol OH, and PG glycerol).

strongly suggest that hydrogen bonding of K246, K247, R73, and R99 with lipid headgroups contributes greatly to the binding energy, along with the FL. The simulations also show that CHOL limits membrane bending, which may slow fusion.

To further examine the importance of K246 and K247 in the

membrane interaction, analogous simulations TT with mutations K246A and K247A. For a interacting with a PC:PG (2:1) membrane, the time during the simulation is shown in Fig. 9a, hydrogen bonds per TT is 38 ± 4. Both the tilt

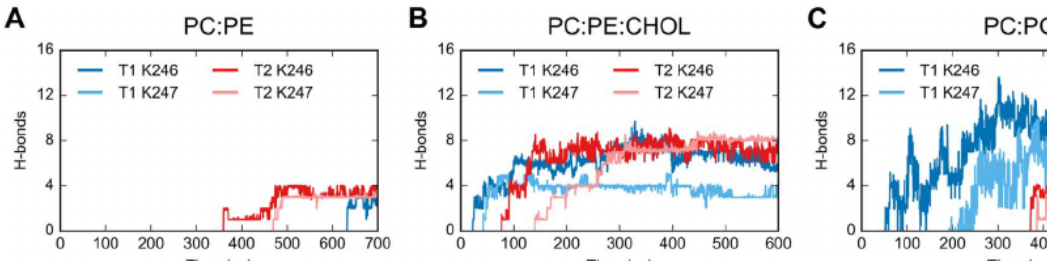

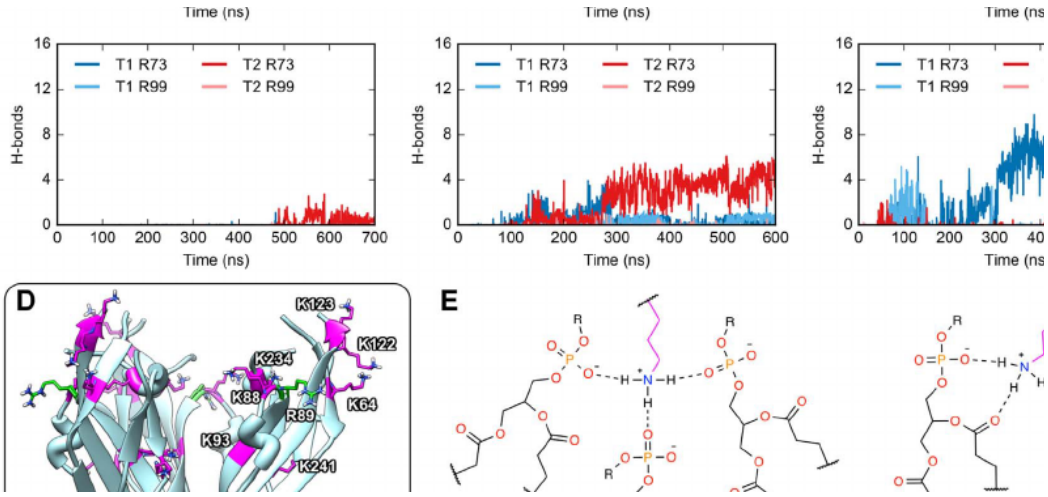

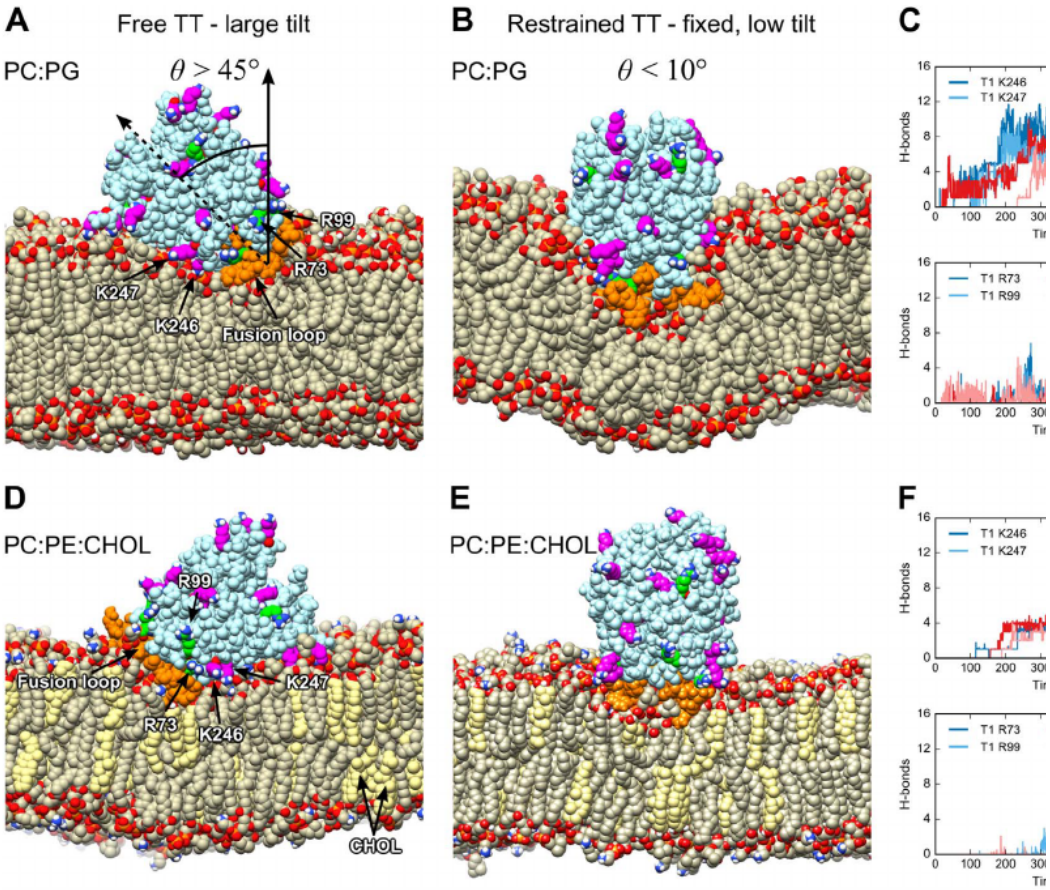

Fig. 8. Simulation cross-section of free (A) and harmonically restrained (B, fixed in vertical orientation, θ < 10°) truncated trimers interacting with F positively-charged resides (K246, K247, R73, R99) near the FL and neighboring lipids. Simulation cross-section of free (D) and harmonically restrained (E) with PC:PE:CHOL. F) Hydrogen bonds of positively-charged resides near the FL and neighboring lipids. Lipid carbon atoms are shown in tan color, choles atoms in cyan except fusion loop (orange), Lys (magenta), and Arg (green) residues. H-bonds between the fixed trimer and neighboring lipids in the PC:PG ca of the membrane (B).

Table 2
Approximate protein-membrane interaction energies (kcal/mol) [a].

Membrane comp.	WT sE TT		K246A/K247A TT mutant	
	All AA[b]	FL AA only	All AA[b]	FL AA only
PC:PE	−1042 ± 28	−464 ± 11	–	–
PC:PE:CHOL	−1693 ± 25	−360 ± 12	−414 ± 18	−373 ± 16
PC:PG	−1768 ± 22	−370 ± 11	−608 ± 25	−536 ± 20
PC:PE:CHOL (fixed tilt)	−880 ± 19	−506 ± 15	−681 ± 22	−564 ± 15
PC:PG (fixed tilt)	−1707 ± 27	−626 ± 11	−809 ± 34	−556 ± 17

[a] Includes all van der Waals interactions and any Coulombic interactions up to 1 nm away from protein.
[b] AA stands for amino acids.

hydrogen bonds formed are strongly reduced compared with the results for wild type TT in Fig. 5. Fig. 9B shows the cross section from a simulation at 700 ns in which K246A/K247A TT was fixed in a vertical

in Fig. 10 for simulations in which the TTs
orientation with respect to the membrane. R

interacting with PC:PE:CHOL and PC:PG, an
interacting with PC:PG. The results show th
membrane in wrapping around the tip of the
interacting with PC:PG corresponds to a signifi
angle. This suggests that hydrogen bond form
K247 and the lipids contributes to destabilizat

4. Discussion

NR provides a high-resolution measureme
tion of Dengue E trimers into lipid bilayers,
surement of the orientation distribution of the
the membrane normal. The NR results show th
which contains the fusion loop, is located at t
headgroups and the hydrophobic tails of the o
insertion is the same for PC:PG:CHOL, PC:PE:

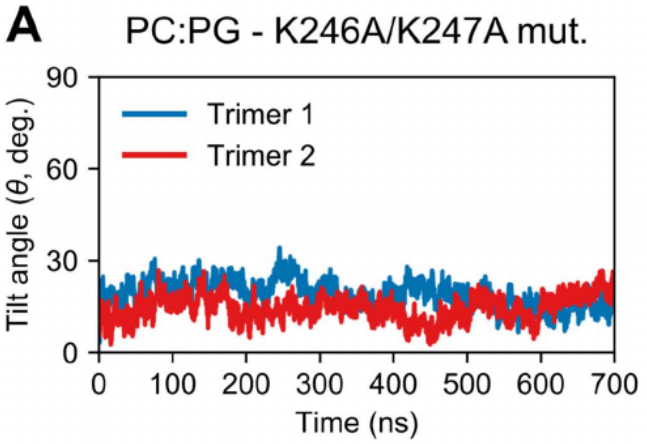

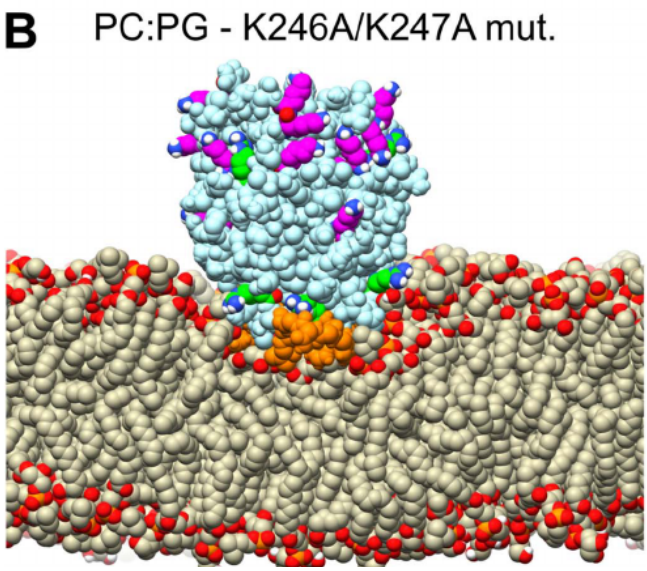

of W101 and F108 with the lipid tails promote
the lipid acyl chain region. Insertion of the
membrane is also promoted by hydrogen bonc
lipid headgroups. An important new insight fr
formation of hydrogen bonds between K246,
phosphate oxygens in the lipid headgroups. K
located near the tip of the trimer in the vici
These interactions induce tilting of the prot
membrane normal as well as deeper insertio
that both CHOL and PG promote protein tilt
mation. This observation is consistent with th
reported trends in binding affinity and in fus
experimental results show little binding affinit
either CHOL or AL, whereas binding affinity
with 30% CHOL and increased even more st
strong dependence of sE binding affinity on th
reported previously [31,33]. Fusion of DV w
been reported to be strongly promoted by AL
binding affinity of sE with membranes [30] a
fusion of flaviviruses [28–30] have been show
content. The experimental finding that the bi
greater for 30% PG than for 30% CHOL in the
that AL promote binding and fusion more stro
mole basis. This is consistent with prior work
dence of fusion on cholesterol in the presence

While our simulations cannot probe the ca
nity) of sE trimers to the membrane due to
length and time scales, they indicate that AL a
H-bonding of TT to the membrane to a similar e
contrasts with the experimental observation c
binding affinity with AL than with CHOL, may
simulations began with the TT in contact with
the experimental study includes the full adsor
cesses. Electrostatic interactions involving AL
sorption of sE to the membrane from solution.

While both PG and CHOL promote the fo
number of hydrogen bonds between sE and the
128 per trimer), their mechanisms of action

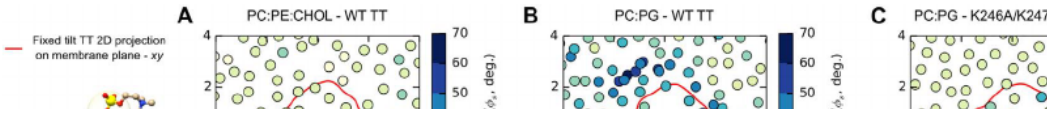

Fig. 9. A) Tilt angle of simulated truncated E trimer K246A/K247A mutant on PC:PG lipid membrane as a function of time. B) Simulation cross-section of truncated E trimer K246A/K247A mutant interacting with PC:PG with fixed protein vertical orientation ($\theta < 10^{\circ}$) with respect to the membrane normal. No significant membrane deformation is observed compared to the wild-type case (Fig. 8B). System was simulated for 700 ns. Color scheme is the same as in Fig. 8.

to the membrane, but rather tilts with respect to the membrane normal (up to 30° under the experimental conditions). The amount of tilt is the same within experimental uncertainty for the three membrane compositions.

The simulations provide atomic resolution as well as insight into the detailed molecular interactions. As expected, hydrophobic interactions

bonding with sE through direct interactions. Tl
PG is a better H-bond donor/acceptor and is les

choline moiety in PC. The net negatively-charg
PG also participate in electrostatic interacti
charged K246, K247, R73, and R99 residues. I
effect is indirect. CHOL resides within the lipi
the distance between the lipid headgroups. Tl
with the well-known condensing effect of CH
While the presence of CHOL in the tails causes
decreasing the cross-sectional area occupied by
of each lipid, the average distance between lip
due to the volume occupied by cholesterol. In
total area divided by the number of phospholi

the PC:PE:CHOL system (67.9 $Å^2$) compared to the PC:PE bilayer (58.3 $Å^2$), whereas the cross-sectional area per lipid for PC:PE:CHOL (45 $Å^2$) is less than that for PC:PE (58 $Å^2$) due to the condensing effect of CHOL. This increased area available per phospholipid headgroup provides greater access to the phosphate oxygens of the lipid headgroups for hydrogen bonding. While the large number of interactions promoted by both PG and CHOL facilitate insertion of the FL into the membrane, the simulations show that rare direct contacts between W101 and CHOL also promote partitioning of this residue within the hydrophobic core of the bilayer. Direct contacts are rare because the location of CHOL within the lipid tails provides little access to CHOL's hydroxyl groups. The finding that direct contacts are rare in the simulations is consistent with the previously reported experimental result that CHOL did not associate strongly enough with E to be labeled by photocholesterol or to coextract with CHOL [32].

The fact the CHOL promotes hydrogen bonding though an indirect mechanism explains the previously enigmatic findings that, in absence of AL, CHOL promotes membrane binding [30,32], lipid mixing [29,30,33], and full fusion [28] despite absence of a strong interaction between CHOL and E [32]. An alternative hypothesis was proposed for the indirect role of CHOL in promoting binding of sE to membranes and for a lack of CHOL dependence in fusion of DV to C6/36 mosquito cells [32]. Note that C6/36 mosquito cells contain AL in the outer membrane. Umshankar et al. proposed that CHOL facilitates clustering and trimerization, and thereby stable membrane binding of sE whereas, in absence of CHOL, sE remains monomeric and the binding energy is insufficient for stable membrane binding. They argued that since E is clustered on virus particles, CHOL is not required for trimerization, stable membrane binding, and fusion, consistent with the lack of CHOL dependence for fusion of DV with C6/36 mosquito cells [32]. While this hypothesis is consistent with the data for membrane binding of sE, it is not consistent with the observation that lipid mixing [29,30,33] and full fusion [28] are promoted by CHOL in flaviviruses in absence of AL. We argue here that the lack of CHOL dependence for fusion of DV with C6/36 mosquito cells is due instead to the presence of high concentrations of AL in these membranes. AL promote hydrogen bond formation more strongly than CHOL such that CHOL has little effect on

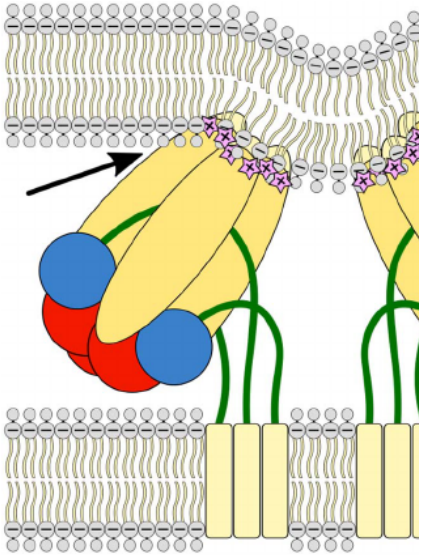

Fig. 12. Illustration showing that a shallow angle (arrows
and the target membrane as domain III and the stem segr
We propose that hydrogen bonds between K246 and K247
at this stage and strongly anchor the trimer into the me
bending. Tilting of the trimers may also promote membra
location of the FL or if the target membrane wraps aroun
Figs. 8 and 9.
(Adapted from [3]).

Fig. 11 [21]. Our simulations show considerabl
formed by R99 in most cases compared to K246
within the FL and may play a role in FL structu
explain the high degree of conservation of that
what stage hydrogen bonding interactions for
and R73 and the lipid headgroups, but there is
they will form at the latter stage of fusion, if r
and the stem segment fold against the body

fusion in the presence of AL. Our simulations showed no evidence for clustering of sE in the presence of CHOL, but such an effect might occur on a much longer timescale.

Regarding the relevance of these new findings to fusion, we note first that a region of positively-charged residues containing at least one lysine near the tip of E is common to nearly all flaviviruses, and that R73 and R99 are also highly conserved among flaviviruses, as shown in

membrane (TM) region of E and target mem approach and a dimple will form in the target

in Fig. 12 [3], creating a shallow angle betwe and the membrane. We propose that hydrog K246, K247, and R73 and the lipid headgro earlier, and provide strong anchoring at th membrane bending. However, the interactions

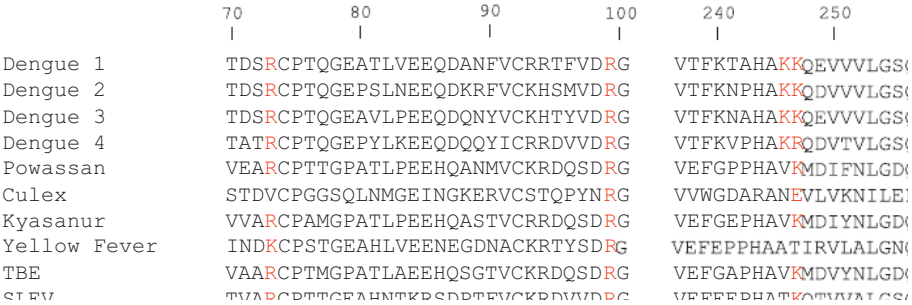

orientational degrees of freedom of E on the surface of the virus are not constrained, E will tilt upon membrane binding to form these interactions as observed for sE in our experimental and simulation studies. If the orientational degrees of freedom of E are constrained and if the membrane of the host cell is sufficiently flexible, upon membrane binding the target membrane will wrap around the tip of the protein and form these interactions as shown in our simulations (Fig. 8B). Such large local deformation of the membrane could serve to promote fusion of the outer leaflet of the host membrane with the viral membrane (Fig. 10).

An alternative hypothesis for the role of AL was proposed previously by Zaitseva et al., wherein AL promote trimerization of E [33]. They concluded that membrane-associated E forms a “restricted hemifusion” (RH) intermediate [54–56] that does not progress to full fusion until AL are present in late endosomes. In their proposed model, upon acidification in early endosomes, dimers of E dissociate and monomers of E insert into the endosomal membrane. They proposed that membrane-associated E remains monomeric in absence of AL, resulting in a structure that does not support mixing of the outer leaflets, and that AL present in late endosomes facilitate trimer formation and progression to fusion. Since the present simulations were performed with trimers rather than monomers, they provide no evidence for or against the hypothesis that AL promote trimerization of E. However, we suggest that AL may simply enhance binding and anchor E into the host membrane sufficiently to support fusion.

Our experimental results showed that in the extreme case of 100% PG, electrostatic or hydrogen bonding interactions with residues along the length of the trimer (K64, K122, K123, K202, K204, K241, K305, K307, K310, K361) are strong enough to dominate over hydrophobic interactions of the tip, and drive the trimers to a side-on orientation. However, for realistic fractions of AL, the tip-inserted conformation results. The fact that strong electrostatic or hydrogen bonding interactions lead to a side-on orientation suggests an important role for the FL in controlling the orientation. Hydrophobic interactions of the FL are important for maintaining a fusion-inducing tip-inserted orientation and avoiding an unproductive side-on orientation.

High conservation of residues in the FL among flaviviruses indicates

than in the simulations (> 60°). One possibl thering of the lipid bilayers may have substan ness of the membrane. Indeed, we did not membrane roughness upon binding, even fo Increased membrane stiffness due to tetherin result to that observed in the fixed orie PC:PE:CHOL. Furthermore, we also note that involved much higher trimer coverages. This strong effect in the NR data. At such high cove %), the trimers may be hindered from tilti crowding of neighboring trimers.

In a prior simulation study, the potential termined for an E trimer as a function of di 70:30 PC:PG membrane [57]. In that work, th perpendicular orientation with respect to the m simulation. The minimum in free energy was Since the present results show that sE is til membrane due to increased hydrogen bonding with phosphate oxygens, we conclude that 15 kcal/mol is a lower limit and the true free substantially greater than that value. Consiste an experimental measurement for an 80:20 PC value of 20 kcal/mol [31].

Finally, we note that K246 and K247 are e the mature virus and therefore may be target significant challenge in finding effective fusi viruses and flaviviruses is that some desirable only become accessible after the pH-dependen occurs within the endosome [45]. The fact t accessible on the surface of the mature virus o feature that may be exploitable for antiviral act the effects of mutating residues K246 and K2 mental studies pose significant challenges. could interfere with the protein's function woul order to conclude that an observed effect of th due to decreased binding affinity. While suc beyond the scope of the present work, we

that the FL is critical to fusion. Based on our results and prior data, we contend that the primary roles of the FL are to ensure insertion of the tip of E and to lower the energy barrier to fusion by destabilizing the target membrane [4]. Prior studies involving peptides comprised of the FL sequence have shown substantial membrane-destabilizing effects [13–15].

In a prior study of the FL of E in tick-borne encephalitus virus, Allison et al. found that mutations to L107 (within the FL) strongly impacted both binding of recombinant subviral particles to and fusion with 1:1:1:1.5 PC:PE:sphingomyelin:CHOL liposomes [23]. While the mutation L107F retained a significant degree of fusion activity, L107T impaired activity and L107D abolished fusion activity. They also showed by liposome coflotation that L107D abolished binding of recombinant subviral particles to the same liposomes. These results may seem to conflict with our conclusion that hydrogen bonding interactions of K246, K247, and R73 dominate the binding interaction over interactions of the FL, even in the absence of AL. However, replacement of L107 with the charged residue (D) will disfavor insertion of the FL into the hydrophobic core of the membrane due to the charged residue and associated water molecules. Since binding of E to CHOL-containing

throughput mutational study of DV serotype 3 equivalent mutations (K244I and K244E in I

levels of wildtype expression, yet virions showe or infectivity, consistent with our proposal [8]

5. Conclusions

Residues K246, K247, and R73 form hydro of lipid headgroups and contribute substantia ergy of trimeric E. These interactions contribut than hydrophobic interactions of the fusion drogen bonding interactions cause the sE trin ientation with respect to the membrane norm creased depth of insertion. Strong interaction o sides of the trimer tip anchors the trimer int continuous contact with the FL likely destabi promotes fusion of the outer leaflets. While th both AL and CHOL, the effect is much greater on a per mole basis. In agreement with prior simulations show that sE does not interact str

Acknowledgments

This work was supported by the Laboratory Directed Research and Development program at Sandia National Laboratories, a multi-mission laboratory managed and operated by National Technology and Engineering Solutions of Sandia, LLC., a wholly owned subsidiary of Honeywell International, Inc., for the U.S. Department of Energy's National Nuclear Security Administration under contract DE-NA-0003525. This work was also supported by NIH grant R01 AI075647 (to M.K.). This work was performed, in part, at the Center for Integrated Nanotechnologies, a U. S. Department of Energy, Office of Basic Energy Sciences user facility at Los Alamos National Laboratory (Contract DE-AC52-06NA25396) and Sandia National Laboratories. We gratefully acknowledge support from the Defense Threat Reduction Agency-Joint Science and Technology Office for Chemical and Biological Defense (IAA number DTRA10027IA-3167). We acknowledge the support of the National Institute of Standards and Technology, U.S. Department of Commerce, in providing the neutron research facilities used in this work. Research was performed in part at the National Institute of Standards and Technology (NIST) Center for Nanoscale Science and Technology. This work was supported by the NIST IMS program “Precision Measurements for Integral Membrane Proteins”. This work used the Extreme Science and Engineering Discovery Environment (XSEDE), which is supported by National Science Foundation grant number OCI-1053575. Specifically, it used the Bridges system, which is supported by NSF award number ACI-1445606, at the Pittsburgh Supercomputing Center (PSC). Certain commercial materials, equipment, and instruments are identified in this work to describe the experimental procedure as completely as possible. In no case does such an identification imply a recommendation or endorsement by NIST, nor does it imply that the materials, equipment, or instrument identified are necessarily the best available for the purpose.

Appendix A. Supplementary data

Supplementary data to this article can be found online at https://

[15] M.N. Melo, F.J.R. Sousa, Fa Carneiro, MaRB Castanho A.T. Da Poian, R. Mohana-Borges, Interaction of the with membranes assessed by NMR: the essential role for membrane fusion, J. Mol. Biol. 392 (2009) 736–
[16] P. Larsson, P.M. Kasson, Lipid tail protrusion in sim tivity of influenza fusion peptide mutants and confo Comput. Biol. 9 (2013) e1002950.
[17] D. Mirjanian, A.N. Dickey, J.H. Hoh, T.B. Woolf, M.J tails plays a central role in barrier crossing during lip 114 (2010) 11061–11068.
[18] I.A. Rodenhuis-Zybert, J. Wilschut, J.M. Smit, Dengu factors modulating infectivity, Cell. Mol. Life Sci. 67
[19] E.G. Acosta, L.B. Talarico, E.B. Damonte, Cell entry (2008) 471–479.
[20] C. Sanchez-San Martin, C.Y. Liu, M. Kielian, Dealing alphaviruses and flaviviruses, Trends Microbiol. 17
[21] V.C. Luca, C.A. Nelson, D.H. Fremont, Structure of postfusion envelope trimer, J. Virol. 87 (2013) 818-
[22] S.J. Seligman, Constancy and diversity in the flavivi (2008) 27.
[23] S.L. Allison, J. Schalich, K. Stiasny, C.W. Mandl, F.X. an internal fusion peptide in flavivirus envelope pro 4268–4275.
[24] A.L. Lomize, I.D. Pogozheva, M.A. Lomize, H.I. Mos interactions in positioning of peripheral proteins in n (2007).
[25] S. Yalovsky, M. Rodriguez-Concepcion, W. Gruissem teins - slipping in and out of membranes, Trends Pla
[26] M.D. Resh, Trafficking and signaling by fatty-acylate Chem. Biol. 2 (2006) 584–590.
[27] R.M. Peitzsch, S. McLaughlin, Binding of acylated p phospholipid vesicles: pertinence to mryistoylated pr 10436–10443.
[28] S.W. Gollins, J.S. Porterfield, pH-dependent fusion be and liposomal model membranes, J. Gen. Virol. 67
[29] J. Corver, A. Ortiz, S.L. Allison, J. Schalich, F.X. He fusion activity of tick-borne encephalitis virus and re a liposomal model system, Virology 269 (2000) 37–
[30] K. Stiasny, C. Koessl, F.X. Heinz, Involvement of lip flavivirus fusion mechanism, J. Virol. 77 (2003) 785
[31] E. La Bauve, B.C. Vernon, D. Ye, D.M. Rogers, C.M. S.B. Rempe, A. Zheng, M. Kielian, A.P. Shreve, M.S. K unbinding energy of strongly-bound membrane-asso Biophys Acta 1858 (2016) 2753–2762.
[32] M. Umashankar, C. Sanchez-San Martin, M. Liao, B. M. Kielian, Differential cholesterol binding by class membrane fusion properties, J. Virol. 82 (2008) 92

doi.org/10.1016/j.bbamem.2018.02.012.

References

[1] S.C. Harrison, Viral membrane fusion, Nat. Struct. Mol. Biol. 15 (2008) 690–698.
[2] M. Kielian, Class II virus membrane fusion proteins, Virology 344 (2006) 38–47.
[3] M. Kielian, F.A. Rey, Virus membrane-fusion proteins: more than one way to make a hairpin, Nat. Rev. Microbiol. 4 (2005) 67–76.
[4] R.M. Epand, Fusion peptides and the mechanism of viral fusion, Biochim. Biophys. Acta 1614 (2003) 116–121.
[5] L. Chernomordik, M.M. Kozlov, Protein-lipid interplay in fusion and fission of biological membranes, Annu. Rev. Biochem. 72 (2003) 175–207.
[6] Y. Modis, S. Ogata, D. Clements, S.C. Harrison, Structure of the dengue virus envelope protein after membrane fusion, Nature 427 (2004) 313–319.
[7] C.Y.H. Huang, S. Butrapet, K.J. Moss, T. Childers, S.M. Erb, A.E. Calvert, S.J. Silengo, R.M. Kinney, C.D. Blair, J.T. Roehrig, The dengue virus type 2 envelope protein fusion peptide is essential for membrane fusion, Virology 396 (2010) 305–315.
[8] E.A. Christian, K.M. Kahle, K. Mattia, B.A. Puffer, J.M. Pfaff, A. Miller, C. Paes, E. Davidson, B.J. Doranz, Atomic-level functional model of dengue virus envelope protein infectivity, Proc. Natl. Acad. Sci. U. S. A. 110 (2013) 18662–18667.
[9] G. Hed, S.A. Safran, Initiation and dynamics of hemifusion in lipid bilayers, Biophys. J. 85 (2003) 381–389.
[10] L. Chernomordik, A. Chanturiya, J. Green, J. Zimmerberg, The hemifusion intermediate and its conversion to complete fusion: regulation by membrane composition, Biophys. J. 69 (1995) 922–929.
[33] E. Zaitseva, S.-T. Yang, K. Melikov, S. Pourmal, L.V. ensures its fusion in late endosomes using compartn Pathog. 6 (2010) e1001131–e1001145.
[34] R. Budvytyte, G. Valincius, G. Niaura, V. Voiciuk, M. Z. Goh, P. Shekhar, F. heinrich, S. Shenoy, M. Losche properties of tethered bilayer lipid membranes with Langmuir 29 (2013) 8645–8656.
[35] A. Zheng, M. Umashankar, M. Kielian, In vitro and portant features of dengue virus pr-E protein interac e1001157.
[36] B.J. Kirby, P.A. Kienzle, B.B. Maranville, N.F. Berk, C.F. Majkrzak, Phase-sensitive specular neutron refl nanometer scale composition depth profile of thin-fi Colloid Interface Sci. 17 (2012) 44–53.
[37] A.G. Kikhney, D.I. Svergun, A practical guide to smal of flexible and intrinsically disordered proteins, FEB
[38] F. Heinrich, M. Losche, Zooming in on disordered s dies of proteins associated with fluid membranes, B (2014) 2341–2349.
[39] J. Penfold, R. Thomas, The application of the specul study of surfaces and interfaces, J. Phys. Condens. M
[40] D.J. McGillivray, G. Valincius, F. Heinrich, J.W.F. R W. Febo-Ayala, I. Ignatjev, M. Losche, J.J. Kasianow *Staphylococcus aureus* alpha-hemolysin channels in t branes, Biophys. J. 96 (2009) 1547–1553 .
[41] F. Heinrich, T. Ng, D.J. Vanderah, P. Shekhar, M. Mi A new lipid anchor for sparsely tethered bilayer lipi

consistent treatment of internal and surface residues in empirical pKa predictions, J. Chem. Theory Comput. 7 (2011) 525–537.
[47] N. Schmid, A.P. Eichenberger, A. Choutko, S. Riniker, M. Winger, A.E. Mark, W.F. van Gunsteren, Definition and testing of the GROMOS force-field versions 54A7 and 54B7, Eur. Biophys. J. 40 (2011) 843–856.
[48] S.-W. Chiu, S.A. Pandit, H.L. Scott, E. Jakobsson, An improved united atom force field for simulation of mixed lipid bilayers, J. Phys. Chem. B 113 (2009) 2748–2763.
[49] H.J.C. Berendsen, J.R. Grigera, T.P. Straatsma, The missing term in effective pair potentials, J. Phys. Chem. 91 (1987) 6269–6271.
[50] S. Pronk, S. Páll, R. Schulz, P. Larsson, P. Bjelkmar, R. Apostolov, M.R. Shirts, J.C. Smith, P.M. Kasson, D. Van Der Spoel, B. Hess, E. Lindahl, GROMACS 4.5: a high-throughput and highly parallel open source molecular simulation toolkit, Bioinformatics 29 (2013) 845–854.
[51] M. Liao, C. Sanchez-San Martin, A. Zheng, M. Kielian, In vitro reconstitution reveals key intermediate states of trimer formation by the dengue virus membrane fusion protein, J. Virol. 84 (2010) 5730–5740.
[52] W.C. Hung, M.T. Lee, F.Y. Chen, H.W. Huang, The condensing effect of cholesterol in lipid bilayers, Biophys. J. 92 (2007) 3960–3967.
[53] Y.-Q. Deng, J.-X. Dai, G.-H. Ji, T. Jiang, H.-J. Wang M. Yu, B.X. Ge, Q.-Y. Zhu, E.-D. Qin, Y.-J. Guo, C.-F. neutralizing monoclonal antibody that recognizes a loop of E protein, PLoS ONE 6 (2011) (e16059-160
[54] L.V. Chernomordik, V.A. Frolov, E. Leikina, P. Bronk of membrane fusion catalyzed by influenza hemagg hemifusion, and lipidic fusion pore formation, J. Cel
[55] E. Zaitseva, A. Mittal, D.E. Griffin, L. Chernomordik phaviruses drives membrane fusion through the same Cell Biol. 169 (2005) 167–177.
[56] G.B. Melikyan, S.A. Brener, D.C. Ok, F.S. Cohen, Inr leaflets control the transition from glycosylphosphati hemagglutinin-induced hemifusion to full fusion, J. 995–1005.
[57] D.M. Rogers, M.S. Kent, S.B. Rempe, Molecular basi sociation for the dengue virus envelope protein, Bioc 1848 (2015) 1041–1052.